HMG Advance Access published July 5, 2013

Human Molecular Genetics, 2013 **1–12**
doi:10.1093/hmg/ddt299

The large non-coding RNA ANRIL, which is associated with atherosclerosis, periodontitis and several forms of cancer, regulates ADIPOR1, VAMP3 and C11ORF10

Gregor Bochenek[1], Robert Häsler[1], Nour-Eddine El Mokthari[2], Inke R. König[3,†], Bruno G. Loos[4,‡], Philip Rosenstiel[1,¶], Stefan Schreiber[1,¶] and Arne S. Schaefer[*]

[1]Institute of Clinical Molecular Biology, Christian-Albrechts-University, Kiel, Germany, [2]University Medical Center Schleswig-Holstein, Biobank popgen, Campus Kiel, Kiel, Germany, [3]Institute for Medical Biometry and Statistics, University of Lübeck, University Medical Center Schleswig-Holstein, Campus Lübeck, Lübeck, Germany and [4]Department of Periodontology, Academic Center for Dentistry Amsterdam (ACTA), University of Amsterdam and VU University Amsterdam, The Netherlands

Received April 25, 2013; Revised and Accepted June 20, 2013

The long non-coding RNA ANRIL is the best replicated genetic risk locus of coronary artery disease (CAD) and periodontitis (PD), and is independently associated with a variety of other immune-mediated and metabolic disorders and several forms of cancer. Recent studies showed a correlation of decreased concentrations of proximal ANRIL transcripts with homozygous carriership of the CAD and PD main risk alleles. To elucidate the relation of these transcripts to disease manifestation, we constructed a short hairpin RNA in a stable inducible knock-down system of T-Rex 293 HEK cell lines, specifically targeting the proximal transcripts EU741058 and DQ485454. By genome-wide expression profiling using Affymetrix HG1.0 ST Arrays, we identified the transcription of ADIPOR1, VAMP3 and C11ORF10 to be correlated with decreased ANRIL expression in a time-dependent manner. We validated these findings on a transcriptional and translational level in different cell types. Exploration of the identified genes for the presence of disaease-associated variants, using Affymetrix 500K genotyping and Illumina custom genotyping arrays, highlighted a region upstream of VAMP3 within CAMTA1 to be associated with increased risk of CAD [rs10864294 $P = 0.015$, odds ratio (OR) = 1.30, 95% confidence interval (CI) = 1.1–1.6, 1471 cases, 2737 controls] and aggressive PD (AgP; $P = 0.008$, OR = 1.31, 95% CI = 1.1–1.6, 864 cases, 3664 controls). *In silico* replication in a meta-analysis of 14 genome-wide association studies of CAD of the CARDIoGRAM Consortium identified rs2301462, located on the same haplotype block, as associated with $P = 0.001$ upon adjustment for sex and age. Our results give evidence that specific isoforms of ANRIL regulate key genes of glucose and fatty acid metabolism.

INTRODUCTION

The long non-coding antisense RNA (lncRNA) *ANRIL* (*CDKN2BAS*) is the best replicated genetic risk factor for coronary artery disease (CAD) (1–6) and periodontitis (PD) (7–10) to date. Additionally, *ANRIL* is independently associated on a genome-wide level with a variety of other diseases such as type 2 diabetes, endometriosis, intracranial aneurysma, megakarypopoiesis (3,9,11–17), as well as with several forms of cancer (18–21). Additional association with Alzheimer's

[*]To whom correspondence should be addressed at: University Medical Center Schleswig-Holstein, Campus Kiel, House 6, Institute of Clinical Molecular Biology, Arnold-Heller-Str. 3, 24105 Kiel, Germany. Tel: +49 4315973882; Fax: +49 4315971842; Email: a.schaefer@ikmb.uni-kiel.de
[†]For The CARDIoGRAM Consortium (for a full list of authors, see Supplementary Material).
[‡]For The European Periodontitis Genetics Consortium (for a full list of authors, see Supplementary Material).
[¶]These authors contributed equally to this work.

disease was reported (22). ANRIL is transcribed and spliced in a complex pattern and a large variety of transcripts exist (23–25). The main transcripts are two short forms, both terminating with polyadenylated exon 13, EU741058 (exons 1, 5, 6, 7, 13) and DQ485454 (exons 1–13), and the long form NR_003529, which lacks exon 13 and terminates with polyadenylated exon 20 (exons 1–20). This chromosomal region carries the highest number of disease-associated variants of the human genome and is dense for predicted enhancers (26,27), indicating a complex regulation. At the chromosomal position of *ANRIL* (chr.9p21.3) also reside the tumor-suppressor genes cyclin-dependent kinase 2A (*CDKN2A*) and 2B (*CDKN2B*), which have a well-described role in cell proliferation and apoptosis, and recently, a *cis*-acting silencing mechanism, mediated by specific *ANRIL* transcripts, was described to negatively regulate *CDKN2A/B* expression via chromatin remodeling (28). Association of the genes *CDKN2A/B* with cancerogenesis is well established but the causal link between *CDKN2A/B* and CAD is missing (29). Moreover, a growing number of alternatively spliced ANRIL isoforms were reported for different cell types (23,24,30–32), with hitherto unknown biological functions. *ANRIL* is regulated at least by STAT1 signaling (26), a pathway that mediates response to inflammation upon stimulation of the pro-inflammatory cytokine interferon gamma, and earlier, we showed that bacterial infection up-regulates *ANRIL* transcription in gingival tissues (8), supporting a role of *ANRIL* in the inflammatory response. Additionally, genome-wide association study (GWAS) lead SNPs of CAD were found to be correlated with the severity of atherosclerosis (25) and this correlation was shown to be independent of most traditional risk factors of CAD (33), indicating a hitherto unknown component of the disease. However, GWAS lead SNPs that were associated with cancer were not in linkage disequilibrium (LD) with the CAD-associated lead SNPs, and are strongly associated with *CDKN2A* and *CDKN2B* expression but not with the expression of *ANRIL* (32). The observations that lead SNPs of different diseases have a different influence on *ANRIL* and *CDKN2A/B* expression indicate different contributions of these SNPs to the modulation of transcripts, which are crucial for the pathogenesis of the different conditions. But how the disease-associated variants of this tissue-specific and alternatively spliced lncRNA translate into different diseases such as CAD, PD, cancer and others has remained unknown. A number of CAD-associated variants at this chromosomal locus were predicted to disrupt annotated transcription factor-binding sites (27). Various studies investigated the association of GWAS lead SNPs of CAD with the expression of *ANRIL*, *CDKN2A* and *CDKN2B* and showed different correlations of the risk haplotype with the expression of these genes in different tissues or cell types, indicating cell type-specific splicing and tissue-specific effects of the risk haplotype (23–25,29,31,32,34,35). The differences between these studies may be related to the usage of different cell types of tissues, to the analysis of different transcriptional isoforms, which are likely to be differentially regulated, or to the sample size of the studies. Furthermore, the modulation of transcript levels might be specific to particular conditions of regulatory activation that are not easily detected. However, there is some consistency among the studies that the risk haplotype is associated with decreased levels of the short, more complex isoform DQ485454, indicating a role of the 5′ exons of ANRIL (23,29,31,34–36) in the disease etiology of CAD and PD. According to the observations that other lncRNAs were shown to be involved in the *trans*-regulation of gene expression (37), we hypothesized a *trans*-regulatory function of the 5′ *ANRIL* transcripts on target genes that are relevant for the disease etiology of CAD and PD. We designed short hairpin RNAs (shRNA) to target polyadenylated exon 13. Thus, we excluded transcripts from the analysis, which carried the distal exons (exons 14–19), and constructed a stable tetracycline-inducible knock-down system in the T-Rex 293 (HEK 293) cell line (a derivative of the human embryonic kidney 293 fibroblast cell line; Supplementary Material).

In the current study, we identified three genes, *ADIPOR1*, *VAMP3* and *C11ORF10*, to be regulated by *ANRIL* in a time-dependent manner. These genes all have a well-described role in fatty acid and glucose metabolism, as well as in inflammation. Two of these loci carried risk variants, which were shared by PD and CAD or PD and other metabolic and inflammatory traits.

RESULTS

Induced knock-down of *ANRIL* is negatively correlated with *CDKN2A/2B* expression and cell proliferation

To identify the time-point of strongest reduction of shRNA-mediated knock-down upon tetracycline incubation, we assessed the transcript levels of ANRIL exon 13 in our inducible knock-down cell system at nine different time-points prior to and upon tetracycline induction by quantitative real-time reverse transcription-PCR (qRT-PCR). Exon 13 transcript levels decreased 4 h after induction and reached a minimum after 48 h, with a 2.4-fold reduction compared with the unstimulated controls. Transcript reduction remained stable for at least 96 h upon induction (Supplementary Material, Fig. S1). To further test the functionality of our construct, we assessed the previously described negative correlation of the concentration of the proximal transcripts of *ANRIL* and *CDKN2A* and -2B expression (28), and quantified *CDKN2A/B* transcript levels prior to and 48 and 96 h upon tetracycline induction. *CDKN2A* and *-2B* activity lagged *ANRIL* repression and showed significantly increased concentration 96 h after induction (*CDKN2A*: 1.5-fold, 96 h upon induction $P = 0.014$, *CDKN2B*: 1.3-fold, 96 h upon induction $P = 0.0017$; Supplementary Material, Fig. S2).

As this transcriptional increase of the cell-cycle inhibitors *CDKN2A* and *-2B* was expected to reduce cellular proliferation, we assessed T-Rex 293 cell proliferation by estimating the number of cells/milliliter over time. Cellular proliferation decreased in the stable transfected cell lines 96 h upon tetracycline incubation (mean cell number: 2.5×10^5 cells/ml) compared with the same transfected cell line without tetracycline incubation (mean 7.4×10^5 cells/ml; Supplementary Material, Fig. S3).

Finally, we analyzed the putative effect of the shRNA on 3′ exons of ANRIL to confirm that the short and long transcript forms are independently regulated in our system. We quantified exon 19 by qRT-PCR in the stable transformed T-Rex 293. Exon 19 was not affected by shRNA expression upon tetracycline induction at any time-point (Supplementary Material, Fig. S4).

ADIPOR1, *VAMP3* and *C11ORF10* are regulated by *ANRIL* transcripts

Following these tests, which proved the functionality of our construct, we employed genome-wide mRNA profiling as pilot experiments to identify transcriptional changes upon tetracycline-induced exon-13 shRNA expression using Affymetrix HG 1.0 ST Arrays as previously published (38). Five replicates were performed at each of the time-points 0, 48 and 96 h upon tetracycline induction. Applying stringent selection criteria [false discovery rate (FDR) $<1\%$, fold change of expression >1.5 at every time-point; no outliers accepted], three transcripts showed significant reduction of transcript levels after 48 and 96 h of induction. These genes were *ADIPOR1* (adiponectin receptor 1), *VAMP3* (vesicle associated membrane protein 3) and *C11ORF10* (chromosome 11 open reading frame 10; Table 1). We subsequently validated these findings in the same cell lines, using qRT-PCR. Upon tetracycline induction, all three genes as well as *ANRIL* exon 13 showed significant reduction of transcript levels after 48 h of tetracycline induction (*ANRIL* $= -2.2$-fold, *ADIPOR1P* $= -2.7$-fold, *VAMP3* $= -4.4$-fold and *C11ORF10* $= -4.2$-fold; Fig. 1). This statistically significant effect was observed 24 h earlier than the observed significant transcript reduction of *CDKN2A/2B* (Supplementary Material, Fig. S2).

Next, we replicated our observation in HeLa cells to exclude false-positive findings due to cell-line-specific artifacts. HeLa cells were transiently transfected with a constitutively expressed shRNA-exon13 knock-down construct, and gene expression was monitored by qRT-PCR 0 and 48 h upon transfection. We observed significantly reduced expression for *ADIPOR1* (1.3-fold), *VAMP3* (1.5-fold) and *C11ORF10* (1.5-fold), compared with untransfected HeLa cells (Fig. 2).

To rule out that our observations were produced by unspecific effects of the shRNA or by tetracycline treatment, we performed qRT-PCR for these genes in T-Rex 293 cells that were stably transfected with a pENTR^{TM}/H1/TO vector, which expressed a non-specific shRNA upon tetracycline induction. No differences in gene expression were observed with and without tetracycline incubation (Supplementary Material, Fig. S5).

To further validate the effects of reduced concentrations of *ANRIL* exon-13 isoforms on the protein abundance of VAMP3, ADIPOR1 and C11ORF10, we performed western blot analysis using our stably transfected T-REX 293 cell line. Seven days upon tetracycline induction, protein abundance of all three genes was reduced compared with the unstimulated controls (Fig. 3).

Genetic analysis of the chromosomal regions of *ADIPOR1*, *VAMP3* and *C11ORF10*

Within the coding regions of *ADIPOR1* and *VAMP3*, no genome-wide SNP association was reported for any disease or trait. However, 3 kilobases (kb) downstream of *VAMP3*, a GWAS on Crohn's disease (CD) reported genome-wide associations with *PER3* (period circadian protein homolog 3) (39); 2 kb upstream of *VAMP3*, the extremely large chromosomal region of *CAMTA1* (calmodulin-binding transcription activator1) is located, spanning >1 megabase and being rich in enhancer elements. A recent study reported suggestive evidence of a large chromosomal region within *CAMTA1* to be associated with periodontal pathogen colonization (40). To search for potential associated disease variants across this chromosomal region, we genotyped the 3′ end of *CAMTA1* (91 kb) and the chromosomal region across *VAMP3*, and *PER3* (466 kb) with 524 SNPs [mean distance 0.9 ± 1.2 kb, minor allele frequency (MAF) $>5\%$], using the immunochip (Illumina, USA). We genotyped 600 German aggressive periodontitis (AgP) cases, and 1440 German population representative controls. At our pre-assigned significance threshold of association, at least two neighboring SNPs with $P < 0.01$, we identified no significant SNP associations within the 3′ end of *CAMTA1*, *VAMP3*, *PER3* and *PARK7*. The region that was described to be associated with periodontal pathogen colonization was not covered by the immunochip, and to test this region for the potential association with AgP, we used Affymetrix 500K Gene Array genotype data of our previous GWAS (41). Within *CAMTA1*, we observed several significant SNP associations in our GWAS data, of which the variants rs10864294 and rs17030881 gave the best association signal (Supplementary Material, Fig. S6). Both SNPs, which are not in LD ($r^2 < 0.8$), are located directly upstream of the region that was described to be associated with periodontal pathogen colonization. The sequences, which span rs10864294, are highly conserved in mammals (not existing in other classes) and the sequences, which span rs17030881, are highly conserved from amphibians to mammals. To increase statistical power, we tested the association in our complete AgP case–control sample of 864 German, Austrian and Dutch AgP cases and 3664 geographically matched healthy controls. rs10864294 was associated with $P = 0.008$ and an odds ratio (OR) $= 1.31$ [95% confidence interval (CI) 1.1–1.6], and rs17030881 was associated with $P = 0.002$, OR $= 4.36$ (95% C.I. 1.5–12.5; Table 2). We validated the associations of these SNPs in 1471 North German non-obese CAD cases (BMI < 30) and 2737 geographically matched healthy controls. In the CAD cases, carriership of rs10864294 was associated with $P = 0.015$, OR $= 1.3$ (95% C.I. $= 1.1$–1.6), and carriership of rs17030881 was associated with $P = 0.009$, OR $= 6.09$ (95% C.I. $= 1.3$–28.7, Table 2). Finally, we performed an *in silico* replication using a meta-analysis of 14 genome-wide association studies of CAD comprising 22 233 individuals with CAD and 64 762 controls of European descent (2). SNP rs10864294 showed poor genotype quality in the overall analysis but was in complete LD ($D' = 1$, Supplementary Material, Table S7) with another SNP, rs2301462, upstream of 760 bp.

Table 1. Top 10 list of genes, which showed the strongest change of transcript levels after 48 and 96 h of tetracycline-induced repression of *ANRIL* transcripts

Chr.	Gene	Change of expression (48 h)	Change of expression (96 h)
1	*VAMP3*	−2.01	−2.46
11	*C11ORF10*	−2.00	−2.72
1	*ADIPOR1*	−1.56	−1.74
23	*MAGT1*	−1.47	−1.74
14	*C14orf129*	−1.43	−1.64
17	*MYO1D*	−1.41	−1.57
1	*LRRC8D*	−1.41	−1.64
11	*PNPLA2*	−1.39	−1.59
1	*C1orf162*	−1.33	−1.68
5	*GNPDA1*	−1.30	−1.52

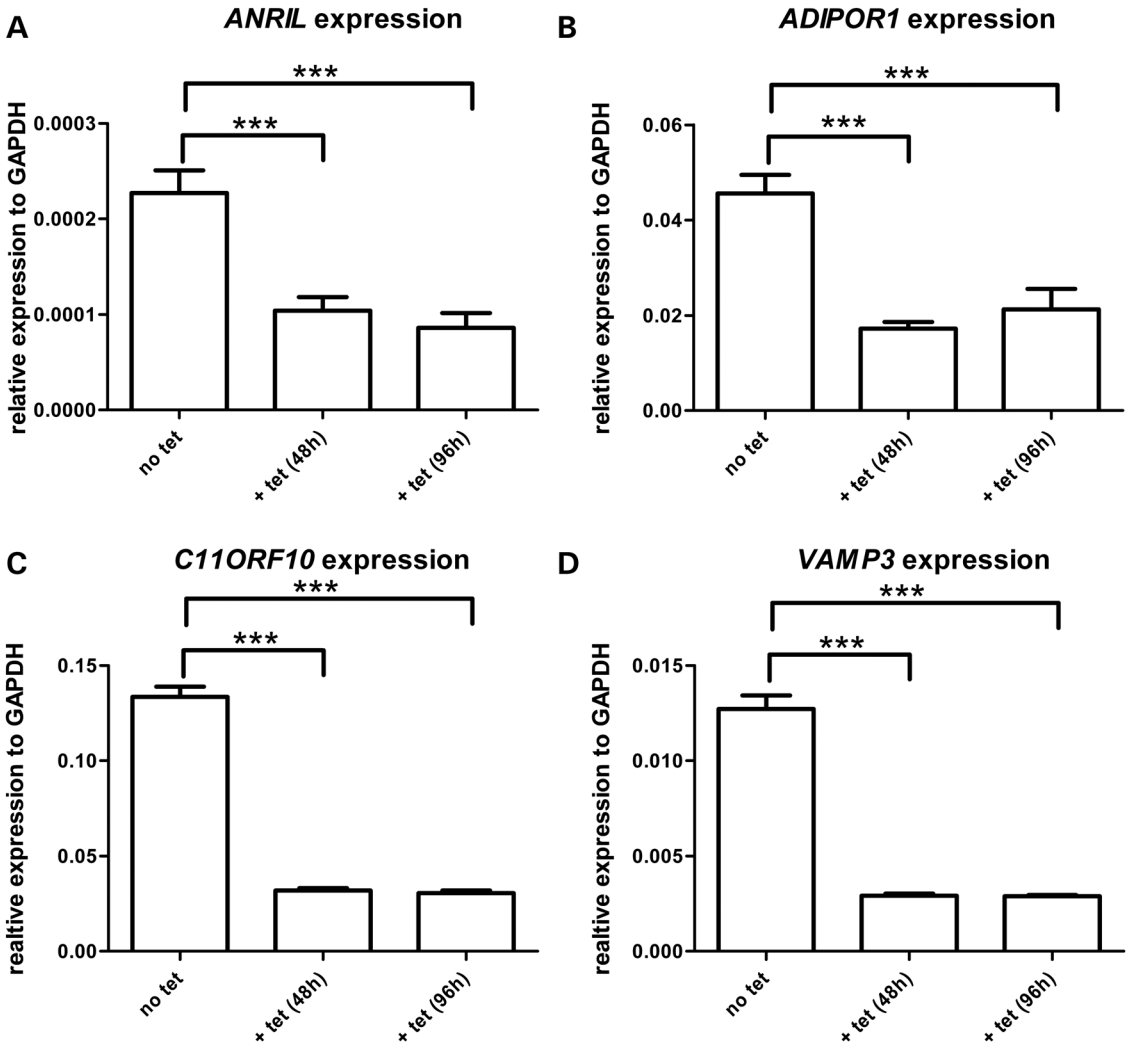

Figure 1. Expression levels of *ANRIL*, *C11ORF10*, *VAMP3* and *ADIPOR1* in stable transformed T-Rex 293 cells 0, 48 and 96 h upon tetracycline induction. shRNA expression was induced by adding 1 μg/ml tetracycline to the medium, and transcript levels were determined after 0, 48 and 96 h. (**A**) Expression of *ANRIL* transcripts (terminating with exon 13) was repressed 2.2-fold ($P = 0.0003$) after 48 h, and 2.6-fold ($P = 0.0001$) after 96 h. (**B**) Expression of *ADIPOR1* was repressed 2.7-fold ($P < 0.0001$) after 48 h and 2.2-fold ($P = 0.0005$) after 96 h. (**C**) Expression of *C11ORF10* was repressed 4.2-fold ($P < 0.0001$) after 48 h and 4.4-fold ($P < 0.0001$) after 96 h. (**D**) Expression of *VAMP3* was repressed 4.4-fold ($P = 0.0001$) after 48 h and 4.4-fold ($P = 0.0002$) after 96 h. Values represent the average of five independent experiments, each performed in triplicate; error bars = standard error of the mean.

In this meta-analysis, rs2301462 was associated with $P = 0.00106$ in an additive genetic model upon adjustment for age and sex.

C11ORF10 locates 7 kb distal to the *FADS* 1-3 (fatty acid desaturases 1-3) gene cluster. A haplotype across *C11ORF9*, *C11ORF10*, *FADS1* and *FADS2* was reported to show genome-wide significant associations with the metabolic syndrome (42), altered phospholipids concentrations (43), T2D (44) and CD (39), but not with CAD. To test this chromosomal region for association with PD, we analyzed variants within *C11ORF9*, *C11ORF10*, *FADS1* and *FADS2* in our German AgP case–control sample, using the immunochip (Table 2). We observed nominal significant association of this haplotype block with our case–control panel of AgP (Table 2, Supplementary Material, Fig. S8) but not with CAD (CARDIoGRAM, data not shown). The best associated SNP (rs1535) was intronic of *FADS2* ($P_{\text{allelic}} = 0.016$, OR = 0.84, 95% CI 0.72–0.98).

For the chromosomal region around *ADIPOR1* (>200 kb), our 500K GWAS data of AgP showed no SNP association. Likewise, no genome-wide association with any disease has been reported for *ADIPOR1*.

The observed co-regulation of *ADIPOR1*, *VAMP3* and *C11ORF10* by ANRIL suggested the existence of shared conserved nucleotide sequences (CNS) of these genes, which could have the potential to serve as binding sites for shared regulatory proteins. To identify such elements, we analyzed the coding sequence of each gene, including additional 2500 bp up- and downstream of the start and stop codon for shared CNS, using the publicly available software tool mVISTA (45). Three CNS of at least 200 bp length and with >70% sequence identity were found to be shared with *ADIPOR1*, *VAMP3* and *C11ORF10*. *VAMP3* and *C11ORF10* shared four CNS (Fig. 4). Several identical transcription factor-binding sites

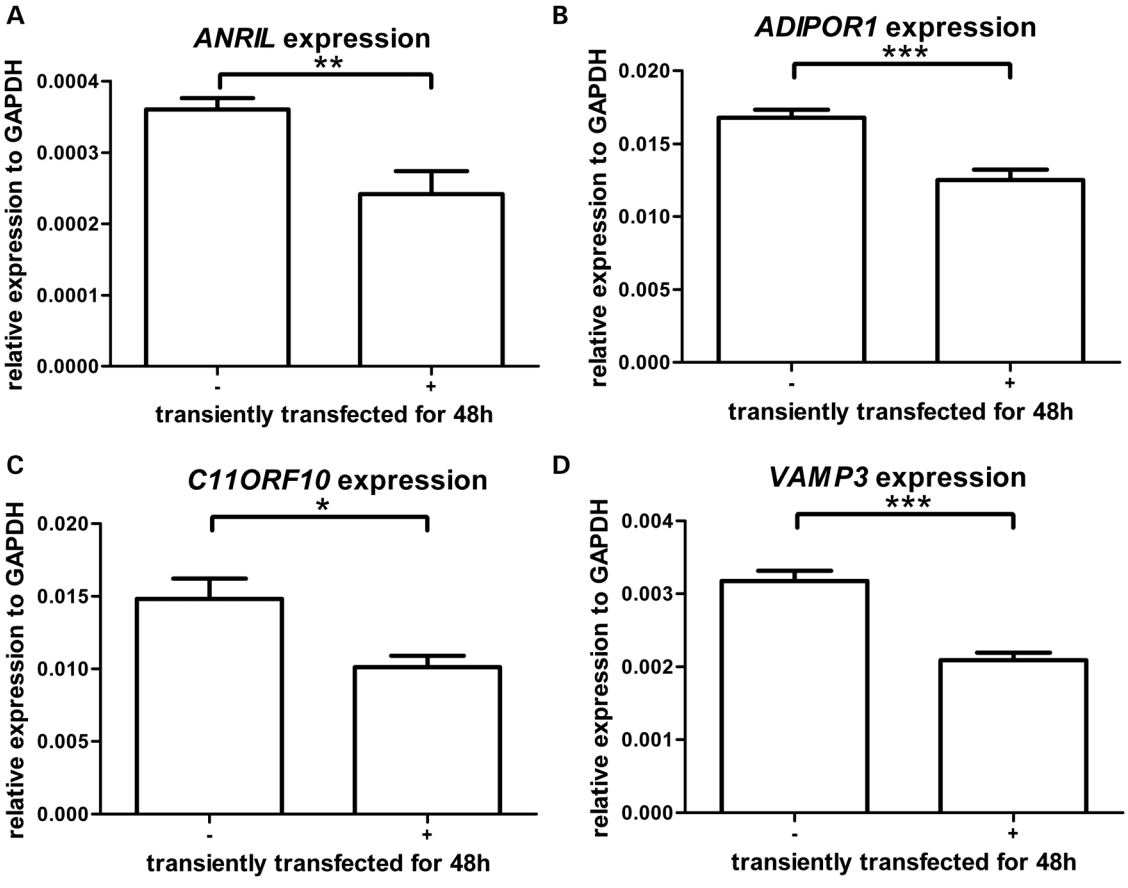

Figure 2. Expression levels of *ANRIL*, *C11ORF10*, *VAMP3* and *ADIPOR1* in transiently transfected HeLa cells 0 and 48 h upon transfection. Transcript levels were determined 0 and 48 h after transfection. (**A**) *ANRIL* expression was repressed 1.5-fold ($P = 0.0053$). (**B**) *ADIPOR1* expression was repressed 1.3-fold ($P = 0.0004$). (**C**) *C11ORF10* expression was repressed 1.5-fold ($P = 0.0114$). (**D**) *VAMP3* expression was repressed 1.5-fold ($P < 0.0001$). Values represent the average of three independent experiments, each performed in triplicate; error bars = standard error of the mean.

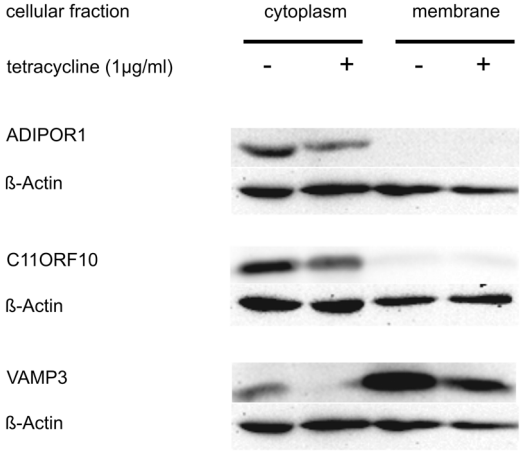

Figure 3. Reduced protein levels of ADIPOR1, C11ORF10 and VAMP3 upon induced knock-down of the distal isoforms of *ANRIL* transcripts. Knock-down of *ANRIL* isoforms terminating with exon 13 led to reduced cellular protein levels of ADIPOR1, C11ORF10 and VAMP3 after 7 days. Whereas ADIPOR1 and C11ORF10 only were detected in the cytoplasm fraction, VAMP3 was also found in the membrane fraction, where protein concentration was also reduced.

were predicted for each of the three CNS that are shared between the three genes (Supplementary Material, Table S4).

Overexpression of *ANRIL* exons 1–5–6–7–13

Our knock-down construct targeted all transcriptional isoforms of ANRIL, which terminated with exon 13, but the full spectrum of alternative isoforms of these transcripts is currently unknown. To study the effects of increased expression of 5′ exons on the identified target genes, we over-expressed a transcript, innate to HUVEC cells (24) and gingival epithelial cells, that incorporated the proximal exons 1–5–6–7–13. Upon 48 h of tetracycline induction, we observed a significant upregulation of ANRIL transcripts, which carried exon 13, as well as of *C11ORF10*. The expression of *ADIPOR1* and *VAMP3* was not significantly altered (Fig. 5).

DISCUSSION

lncRNAs were previously shown to be involved in the *trans*-regulation of the expression of distant genes (37,46). Our data suggest that decreased expression of *ANRIL* transcripts containing exon 13 is correlated with decreased expression levels of *ADIPOR1*, *VAMP3* and *C11ORF10*. However, we did not give

Table 2. Association statistics for SNPs within *CAMTA1* and *C11orf9*, *C11ORF10*, *FADS1* and *FADS2*

Chr.	Gene	SNP	*P*-value (allelic)	OR (95% CI)	Cases MAF %	N11 (F11)	N12 (F12)	N22 (F22)	Controls MAF %	N11 (F11)	N12 (F12)	N22 (F22)
Chr. 1	*CAMTA1*	rs10864294 (CAD)*	**0.015**	1.30 (1.1–1.6)	8.22	1241 (84.38)	218 (14.81)	12 (0.82)	7.14	2359 (86.19)	365 (13.34)	13 (0.47)
		rs10864294 (AgP)**	**0.008**	1.31 (1.1–1.6)	9.20	717 (82.41)	146 (16.78)	7 (0.81)	7.32	3165 (85.98)	493 (13.39)	23 (0.63)
		rs17030881 (CAD)*	**0.009**	6.09 (1.3–28.7)	0.27	1476 (99.46)	8 (0.54)	0 (0)	0.04	2248 (99.91))	2 (0.09)	0 (0)
		rs17030881 (AgP)**	**0.002**	4.36 (1.5–12.5)	0.41	855 (99.19)	7 (0.81)	0 (0)	0.09	3728 (99.81)	7 (0.19)	0 (0)
		rs2301462 (CARDiOGRAM)	**0.001**	1.04 (1.02–1.07)								
Chr. 11	*C11ORF9*	rs174535#	**0.040**	0.86 (0.8–0.99)	31.50	277 (46.17)	268 (44.67)	55 (9.17)	34.84	608 (42.19)	662 (45.94)	171 (11.87)
		rs174537	**0.036**	0.86 (0.7–0.99)	30.92	281 (46.83)	267 (44.50)	52 (8.67)	34.32	620 (43.03)	653 (45.32)	168 (11.66)
	C11ORF10	rs102275##	**0.047**	0.86 (0.8–0.99)	31.42	279 (46.50)	265 (44.17)	56 (9.33)	34.64	611 (42.46)	659 (45.80)	169 (11.74)
		rs174547###	**0.025**	0.85 (0.73–0.98)	30.83	282 (47.00)	266 (44.33)	52 (8.67)	34.46	615 (42.77)	655 (45.55)	168 (11.68)
	FADS1	rs174550+	**0.025**	0.85 (0.7–0.98)	30.83	282 (30.83)	266 (47.00)	52 (8.67)	34.46	616 (42.75)	657 (45.59)	168 (11.66)
	FADS2	rs1535◇	**0.016**	0.84 (0.7–0.97)	30.67	283 (47.17)	266 (44.33)	51 (8.50)	34.58	613 (42.57)	658 (45.69)	169 (11.74)

Bold letters depict significant SNP associations; allelic, allelic test; F, frequency; 11, homozygous carriers of the common allele; 12, heterozygous carriers; 22, homozygous carriers of the rare allele. Chr. 1: *1471 CAD cases (BMI < 30) were recruited in North Germany (Schleswig-Holstein) and matched with population representative controls ($n = 2737$) of the same geographical region. **AgP cases were recruited across Germany ($n = 631$), Vienna ($n = 69$) and the Netherlands ($n = 164$) and matched with the same German controls as for CAD, and additional PD-free controls from southern Germany, Bavaria ($n = 559$), and from the Netherlands ($n = 368$). SNP rs10864294 showed poor genotype quality in a meta-analysis of 14 genome-wide association studies of CAD comprising 22 233 individuals with CAD and 64 762 controls of European descent but was in complete LD with rs2301462 (Supplementary Material, Table S7). The *P*-value of rs2301462 was adjusted for age and sex in this meta-analysis. Chr. 11: Genome-wide associations with #lipid metabolism, CD, metabolic syndrome; ##lipid metabolism, metabolic traits, resting heart rate; +type 2 diabetes, lipid metabolism; ◇lipid metabolism, metabolic syndrome, response to statin therapy (see references in the text). Six hundred German AgP cases and 1441 German population representative controls were genotyped using the Immunochip (Illumina).

direct evidence for the interaction of *ANRIL* transcripts with the transcriptional complex of the identified target genes. Because the expression of specific *ANRIL* transcripts and *CDKN2A/2B* is co-regulated through usage of the same transcriptional start site (28), it can be argued that the effects, which were observed in our study, may be mediated through antisense transcription regulation of *CDKN2A/2B*. However, our data showed a transcriptional response of *ADIPOR1*, *VAMP3* and *C11ORF10* 24 h earlier compared with the *cis*-regulated genes *CDKN2A/2B*. Likewise, other studies repeatedly showed that the effects of sequence variants acting in *cis* were stronger for *ANRIL* than for *CDKN2A/2B* expression (25,29,31,32). A late significant impact on the transcriptional regulation of *CDKN2A* and *-2B* upon shRNA induction was also observed for other antisense ANRIL transcripts, which showed increasing effects with longer intervals of antisense expression (24 cell passages compared with 12 cell passages) (28). This study also gave evidence that ANRIL RNA participates directly in the regulation of chromatin structure. It is possible, although highly speculative, that ANRIL regulation of the identified target genes is mediated by transcription factors instead of the regulation of chromatin structure. These different mechanisms could result in different reaction times to shRNA gene silencing. Further support for a direct role of ANRIL transcripts on distant target genes was obtained by the overexpression experiment of our own study. The vector, which inducibly over-expressed the short ANRIL transcript form EU741058 (exons 1–5–6–7–13), integrated randomly into the genome. Interestingly, we saw an effect only on *C11ORF10* transcript levels. The fact that we did not observe an increase of *ADIPOR1* and *VAMP3* transcript levels could be attributable to unknown position effects, or, that transcripts other than EU741058 were required for specific regulation of these target genes. Generally, the usage of different exons may confer different biological functions to different isoforms, and the increasing number of different and cell-type-specific ANRIL transcripts that are being discovered (23,24,31) indicate such functions also for ANRIL transcript forms. Experiments which overexpress other transcripts will be able to test this hypothesis.

ADIPOR1 is a high-affinity receptor for globular adiponectin, a hormone which, e.g., mediates AMPK and PPAR-alpha ligand activities (47), key regulators of fatty acid oxidation and regulation of glucose levels. A negative correlation of body fat and adiponectin levels is well established (48,49). Apart from the function of globular adiponectin to increase fatty acid oxidation, it also strongly increases insulin's ability to stimulate glucose uptake through increased glucose transporter 4 (GLUT4) gene expression and increased GLUT4 recruitment to the plasma membrane (50,51). The hormone plays a role in type 2 diabetes and atherosclerosis, where it may also attenuate the inflammatory response associated with, e.g., atherogenesis (52) and PD (53). In this context, adiponectin is found to act as an anti-inflammatory signal by selectively increasing tissue inhibitors of metalloproteinases (54). It was further established that adiponectin suppresses phagocytic activity and lipopolysaccharide-induced TNF (tumor necrosis factor) expression (55). VAMP3 belongs to the VAMP/synaptobrevin family and plays a role in phagocytosis, where VAMP3 mediates delivery of TNF-alpha to the cell surface of the phagocytic cup, resulting in a subsequent release of TNF-alpha (56). Interestingly,

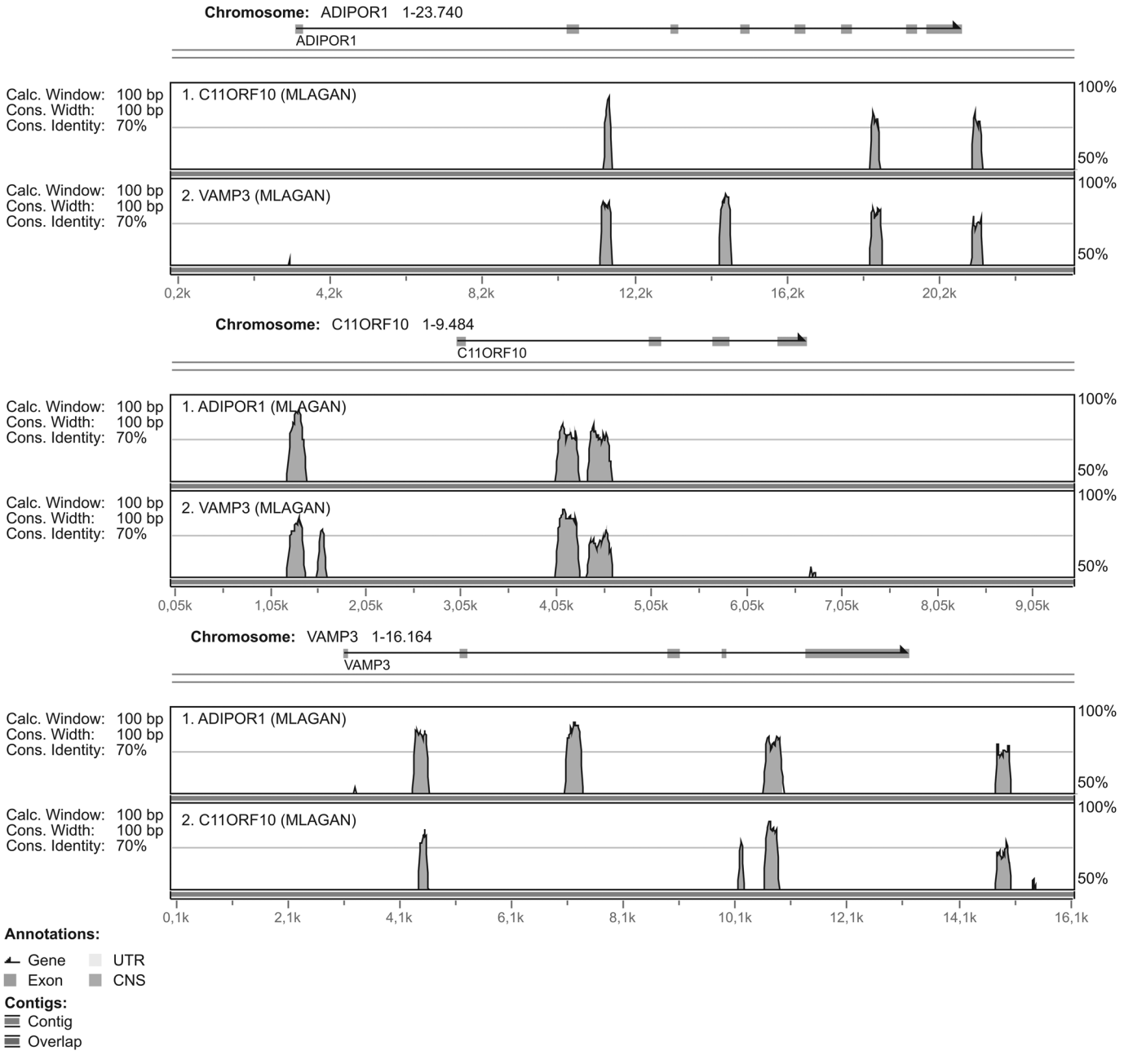

Figure 4. Shared conserved nucleotide sequences (CNS) at *ADIPOR1*, *C11ORF10* and *VAMP3*. Each diagram shows the reference gene plus a chromosomal region of ±2.5 kb in the upper panel. The peaks below indicate chromosomal positions of sequences showing a minimum length of 100 bp with at least 70% homology with the annotated genes. The height of the peaks represents the CNS similarity, whereas the width corresponds to the length of the identified CNS.

VAMP3 is also involved in GLUT4-mediated glucose metabolism. Elevated insulin levels induce translocation of GLUT4 to the plasma membrane to aid glucose utilization, which is mediated by VAMP3 (57,58). Although the function of *C11ORF10* is currently unknown, the genetic region across *C11ORF9*, C11ORF10 and *FADS1-2* is associated with various metabolic traits such as the metabolic syndrome, a cluster of cardiovascular and periodontal risk factors that include obesity, impaired glucose tolerance and type 2 diabetes. *C11ORF10* is furthermore independently genome-wide-associated with inflammatory bowel disease (39).

The effects of homozygous carriership of the CAD main-associated SNPs on the development of CAD were shown to be independent of traditional cardiovascular risk factors and scores (1). Interestingly, a recent case–control and prospective study showed an almost complete reduction of the effect of homozygous carriership of the CAD main-associated SNPs on the development of CAD in the context of a diet high in raw vegetable intake but low in fat (59). Furthermore, interaction of 9p21.3 variants and glycosylated hemoglobin, a marker of hyperglycemia, on coronary heart disease in individuals with type 2 diabetes was reported (60). In this study, the genetic effect of 9p21.3 variants on CAD

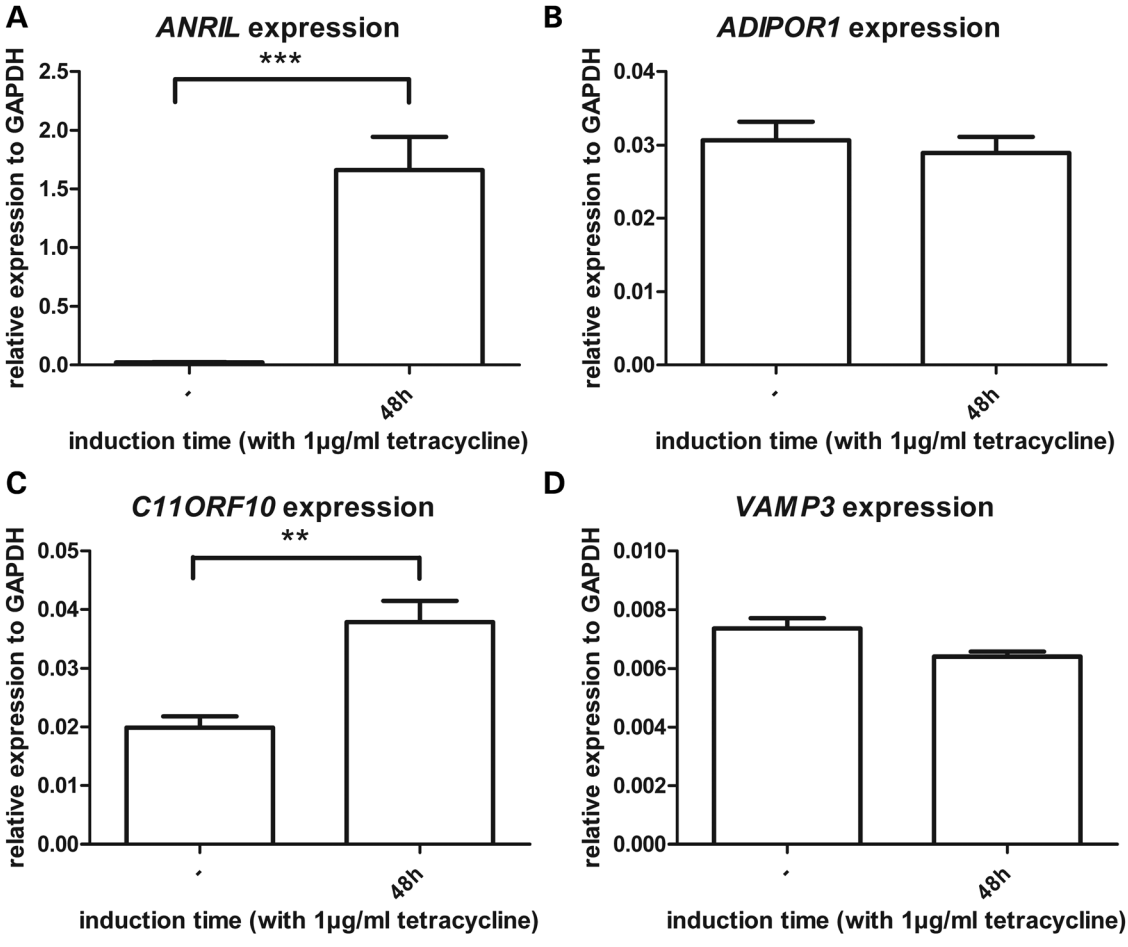

Figure 5. Expression levels of *ANRIL*, *C11ORF10*, *VAMP3* and *ADIPOR1* in stable transformed T-Rex 293 cells 0 and 48 h upon tetracycline-induced overexpression of short variant containing exon 1–5–6–7–13 (EU741058). Transcript expression was induced by adding 1 µg/ml tetracycline to the medium and transcript levels were determined after 0 and 48 h. (**A**) Expression of *ANRIL* transcripts (terminating with exon 13) was increased 75-fold ($P = 0.0002$) after 48 h. (**B**) Expression of *ADIPOR1* was not affected by increased ANRIL levels after 48 h. (**C**) Expression of *C11ORF10* was increased 1.9-fold ($P = 0.0014$) after 48 h. (**D**) Expression of *VAMP3* did not significantly change after 48 h. Values represent the average of five independent experiments, each performed in triplicate; error bars = standard error of the mean.

was found to be magnified in the presence of poor glycemic control. However, recent data of the Framingham Heart Study showed no evidence for the association of the CAD risk haplotype (rs1333049) with traditional CAD risk factors such as cholesterol and low-density lipoprotein (LDL) (34). One potential explanation is that the modulation of the concentration of these metabolites may be specific to particular conditions that are not easily detected in cross-sectional surveys. In this context, it was also discussed that there is a complex regulatory space at the chr.9p21.3 locus and that disease-associated alleles may have condition-specific effects (26).

Interestingly, carriership of the risk C allele of the GWAS lead SNP rs1333049 is comparatively common in both European and Asian populations (MAF HapMap-CEU = 49.2%, HapMap-HCB = 47.8%, HapMap-JPT = 51.1%), where homozygosity even seems to be balanced for both alleles (HapMap-CEU: CC = 22.0%, TT = 23.7%; HapMap-JPT: CC = 26.7%, TT = 24.4%), whereas in Sub-Sahara populations the C-allele is comparatively rare (HapMap-YRI 17.5%, CC = 1.7%). Interestingly, a similar enrichment of the risk-associated alleles of the haplotype block spanning the genes *C11ORF9-10* and *FADS1-2* was observed for European (MAF HapMap-CEU = 34%) and Asian populations (MAF HapMap-HCB = 34%, HapMap-JPT = 31%) compared with the Sub-Saharan population (MAF HapMap-YRI = 11%), where no homozygous carriers of the rare alleles were observed. The correlation of low frequencies of these risk haplotype blocks in Sub-Sahara populations together with the role of ANRIL transcripts on ADIPOR1, VAMP3 and C11ORF10 protein levels described in the current study might be interesting in the context of earlier observations that found LDL cholesterol and apolipoprotein B levels in westernized Africans to be significantly lower in black neonates when compared with white neonates (61).

Interestingly, also strong differences in MAF for rs10864294 upstream of *VAMP3*, which we showed to be increased in CAD patients and AgP cases, were observed between European and Asian populations, and Sub-Sahara populations (HapMap-CEU = 7.5%, HapMap-JPT = 5.3%, HapMap-YRI = 51.3%). In conclusion, our findings place specific *ANRIL* transcripts, which are modulated by the main

CAD- and PD-associated haplotype, into a regulatory network that integrates glucose and fatty acid metabolism and immune response, and add important pieces to the yet-unassembled puzzle of the molecular role of *ANRIL* transcripts in the etiology of these diseases. Future identification of the exact transcript forms of *ANRIL* that mediate the expression of the described target genes and the identification of the putative RNA-binding proteins will help to further understand the molecular function of *ANRIL*. Other haplotypes are independently associated with increased susceptibility to other diseases such as diabetes and cancer. The systematic elucidation of the full spectrum of transcripts that are modulated by these variants and the characterization of their biological functions will help to identify the regulatory networks that play a role in the etiology of such different diseases such as cancer, T2D, CAD, PD and Alzheimer, which are all connected by this differentially spliced lncRNA.

MATERIALS AND METHODS

Ethics statement

Written informed consent was obtained from all participants and the recruitment and the experimental protocols were approved by the institutional ethics review board and data protection authorities.

Study population

For detailed descriptions of the component studies, see Supplementary Material.

Construction of a stable tetracycline-inducible shRNA knock-down or overexpression system in T-Rex 293 (HEK 293) cell lines

For a detailed description on the PCR conditions, primer sequences and protocols, see Supplementary Material. In brief, single-stranded DNA oligonucleotides were designed using the manufacturer's software RNAi Designer (www.invitrogen.com/rnai). Double-stranded oligonucleotides were annealed and cloned into the pENTR^{TM}/H1/TO vector according to the manufacturer's instructions (Invitrogen, USA). To generate a stable cell line, the pENTR^{TM}/H1/TO construct was transfected into T-REX 293 cells using FuGene (transfection reagent, Promega), according to the manufacturer's protocol (Promega, USA). Six hours after transfection, the medium was removed and replaced with fresh growth medium (DMEM+10% FCS, Life Technologies, USA). Cells were incubated over night at 37°C. The following day, cells were replaced to a larger sized tissue culture format with fresh growth medium containing Blasticidin (5 μg/ml) and Zeocin (100 μg/ml). The medium was replaced with fresh growth medium containing Blasticidin and Zeocin every 3 days until Blasticidin- and Zeocin-resistant colonies were selected (14 days after transfection). Twelve Blasticidin- and Zeocin^{TM}-resistant colonies were selected and taken into further cultivation. The same selection procedure was done for the overexpression system, where the transcript containing exons 1–5–6–7–13 was cloned in the pcDNA4/TO vector.

Analysis of cell proliferation

Cell proliferation of T-Rex 293 cells was estimated by counting the number of cells/milliliter over time (cellometer auto T4 counter, Nexcelom Bioscience, USA). In brief, six 10 ml dishes were plated with a liquid culture medium containing T-REX cells (carrying the stably integrated shRNA targeted to exon 13 of *ANRIL*) with a density of 5.5×10^5 cells/ml. To induce the expression of the shRNA, the growth medium was supplemented with 1 μg/ml tetracycline for three plates, whereas the remaining three plates were not supplemented with tetracyclin. Plates/cells were split every third day and cell number/milliliter was determined with the cellometer auto T4 counter for each plate in triplicates. The same procedure was repeated for T-REX cells, which were not stably transfected with shRNA against exon 13.

Transfection of HeLa cells

For transient transfection, HeLa cells were grown in 10 ml culture dishes until 60% confluency. Cells were transfected with the pENTR^{TM}/U6 construct using FuGene (transfection reagent, Promega) according to the manufacturer's protocol (Promega). Six hours after transfection, the medium was removed and replaced with fresh growth medium (DMEM+10% FCS, Life Technologies).

Genome-wide transcriptome profiling

Total RNA was isolated, processed and hybridized to Affymetrix Human Gene 1.0 ST Arrays according to the manufacturer's instructions. Data were normalized using the open-source software RMA (R, Bioconductor, USA). Fold changes were calculated based on the ratios of the medians, and FDRs were estimated using a Westfall–Young permutation as described in the 'Wiley Series in Probability and Mathematical Statistics', *Resampling-Based Multiple Testing: Examples and Methods for P-Value Adjustment* by Peter Westfall and Stanley Young (New York, 1993), with 5000 permutations. Transcripts were considered differentially expressed when the FDR was $\leq 1\%$ and no outlier was identified (62). Outliers were defined as transcripts with relative expression values that are located within the range of the other experimental group when comparing two experimental groups. Cluster analysis was performed using the TIBCO Spotfire IBD software (Tibco, USA) employing correlation as a distance measure. Five replicates were performed for each of the time-points 0, 48 and 96 h.

Western blot

shRNA expression targeting exon 13 was induced by tetracycline incubation for 7 days. Growth medium was changed every third day. Cells were fractionated in ctyosolic and membrane fraction as follows. Cells grown in 10 ml dishes were washed with cold PBS and 500 μl of cold buffer A (10 mM HEPES, pH 7.9, 10 mM KCl, 1.5 mM $MgCl_2$, 10 mM NaF, phosphatase and protease inhibitor). Plates were scraped, placed into a 1.5 ml tube and incubated at 4°C for 10 min. Lysate was passed through 26 G needle 15 times using a 1 ml syringe and centrifuged for 10 min with 1000*g* at 4°C. Supernatant was removed and centrifuged an additional time for 45 min with 16 000*g* at 4°C. Next, the

supernatant was removed as cytosolic fraction, whereas the pellet was washed with buffer A, and resuspended in RIPA buffer (20 mM Tris–HCl, pH 7.5, 150 mM NaCl, 0.1% SDS, 0.5% sodium deoxycholate, 1% NP-40, phosphatase and protease inhibitor) as membrane fraction. Cytosolic and membrane fractions of tetracycline-stimulated and -unstimulated controls were separated by electrophoresis, and western blotting was performed following standard protocols.

Genotyping and statistical analysis

Genotypes for the chromosomal regions of *VAMP3* and *C11ORF10* and additionally, 91 kb of the downstream part of *CAMTA1* were generated using the custom genotyping array Immunochip (Illumina). The genotypes were automatically called using the GenomeStudio Data analysis software package with the integrated GenCall algorithm (Illumina). All raw genotyping data were combined for clustering and quality control according to the manufacturers instructions. SNPs failed with a call rate $<98\%$ and/or cluster separation score <0.4 were excluded. The final sample size for the explorative part of the study was 600 AgP cases and 1441 controls. SNPs with an MAF $<5\%$ were filtered and removed prior to the analysis.

Genotypes for *CAMTA1* and *ADIPOR1* were generated with the Affymetrix Gene Chip Human Mapping 500K Array Set. Controls were genotyped with the Affymetrix Gene Chip 5.0. SNPs with a genotype call rate $<90\%$ were excluded. GWAS genotype data were automatically called by the BRMBLL algorithm. Genotyping of rs17030881 and rs10864294 (*CAMTA1*) was additionally performed using the TaqMan Genotyping System (Applied Biosystems, USA) on an automated platform, employing TECAN Freedom EVO and 96-well and 384-well TEMO liquid-handling robots (TECAN, Switzerland). All markers were tested for deviations from Hardy–Weinberg equilibrium in controls before inclusion into the analyses ($P = 0.05$).

Genotypes were analyzed using the PLINK v2.049 software (63). Significance of association with single-locus genotypes was assessed using $\chi 2$ tests for allelic 2×2 contingency tables. We used genotype, dominant, multiplicative and recessive genetic models to assess the genetic effect of the associated alleles. LD measures and haplotypes were calculated with HaploView 4.2 (64).

Details of the *in silico* replication in the CARDIoGRAM Consortium have been reported elsewhere (2).

SUPPLEMENTARY MATERIAL

Supplementary Material is available at *HMG* online.

ACKNOWLEDGEMENTS

The contributions of the following researchers and technicians are gratefully acknowledged: Andre Franke, Michael Wittig, Sandra Greve, Tanja Henke, Ines Spitzer, Ilona Urbach, Tanja Wesse and Tanja Kacksteen. Further acknowledged are the contributions of the information specialists of the Biobank popgen: Ulrike Harney and Lukas Tittmann.

Conflict of Interest statement. None declared.

FUNDING

This work was supported by a research grant of the 'Research Center Inflammation Medicine' of the Medical Faculty, Christian-Albrechts-University, University Medical Center Schleswig-Holstein, Campus Kiel (A.S.S. and G.B.), by a grant of the DGP GABA Forschungsförderung (2010) and by a grant of the Deutsche Forschungsgemeinschaft (KFO208) (A.S.S. and G.B.). The funders had no role in study design, data collection and analysis, decision to publish or preparation of the manuscript.

REFERENCES

1. Samani, N.J., Erdmann, J., Hall, A.S., Hengstenberg, C., Mangino, M., Mayer, B., Dixon, R.J., Meitinger, T., Braund, P., Wichmann, H.E. *et al.* (2007) Genomewide association analysis of coronary artery disease. *N. Engl. J. Med.*, **357**, 443–453.
2. Schunkert, H., Konig, I.R., Kathiresan, S., Reilly, M.P., Assimes, T.L., Holm, H., Preuss, M., Stewart, A.F., Barbalic, M., Gieger, C. *et al.* (2011) Large-scale association analysis identifies 13 new susceptibility loci for coronary artery disease. *Nat. Genet.*, **43**, 333–338.
3. WTCCC (2007) Genome-wide association study of 14,000 cases of seven common diseases and 3,000 shared controls. *Nature*, **447**, 661–678.
4. Helgadottir, A., Thorleifsson, G., Manolescu, A., Gretarsdottir, S., Blondal, T., Jonasdottir, A., Sigurdsson, A., Baker, A., Palsson, A., Masson, G. *et al.* (2007) A common variant on chromosome 9p21 affects the risk of myocardial infarction. *Science*, **316**, 1491–1493.
5. McPherson, R., Pertsemlidis, A., Kavaslar, N., Stewart, A., Roberts, R., Cox, D.R., Hinds, D.A., Pennacchio, L.A., Tybjaerg-Hansen, A., Folsom, A.R. *et al.* (2007) A common allele on chromosome 9 associated with coronary heart disease. *Science*, **316**, 1488–1491.
6. Deloukas, P., Kanoni, S., Willenborg, C., Farrall, M., Assimes, T.L., Thompson, J.R., Ingelsson, E., Saleheen, D., Erdmann, J., Goldstein, B.A. *et al.* (2013) Large-scale association analysis identifies new risk loci for coronary artery disease. *Nat. Genet.*, **45**, 25–33.
7. Schaefer, A.S., Bochenek, G., Manke, T., Nothnagel, M., Graetz, C., Thien, A., Jockel-Schneider, Y., Harks, I., Staufenbiel, I., Wijmenga, C. *et al.* (2013) Validation of reported genetic risk factors for periodontitis in a large-scale replication study. *J. Clin. Periodontol.*, **40**, 563–572.
8. Schaefer, A.S., Richter, G.M., Dommisch, H., Reinartz, M., Nothnagel, M., Noack, B., Laine, M.L., Folwaczny, M., Groessner-Schreiber, B., Loos, B.G. *et al.* (2011) CDKN2BAS is associated with periodontitis in different European populations and is activated by bacterial infection. *J. Med. Genet.*, **48**, 38–47.
9. Schaefer, A.S., Richter, G.M., Groessner-Schreiber, B., Noack, B., Nothnagel, M., El Mokhtari, N.E., Loos, B.G., Jepsen, S. and Schreiber, S. (2009) Identification of a shared genetic susceptibility locus for coronary heart disease and periodontitis. *PLoS Genet.*, **5**, e1000378.
10. Ernst, F.D., Uhr, K., Teumer, A., Fanghanel, J., Schulz, S., Noack, B., Gonzales, J., Reichert, S., Eickholz, P., Holtfreter, B. *et al.*. (2010) Replication of the association of chromosomal region 9p21.3 with generalized aggressive periodontitis (gAgP) using an independent case-control cohort. *BMC Med. Genet.*, **11**, 119.
11. Gieger, C., Radhakrishnan, A., Cvejic, A., Tang, W., Porcu, E., Pistis, G., Serbanovic-Canic, J., Elling, U., Goodall, A.H., Labrune, Y. *et al.* (2011) New gene functions in megakaryopoiesis and platelet formation. *Nature*, **480**, 201–208.
12. Saxena, R., Voight, B.F., Lyssenko, V., Burtt, N.P., de Bakker, P.I., Chen, H., Roix, J.J., Kathiresan, S., Hirschhorn, J.N., Daly, M.J. *et al.* (2007) Genome-wide association analysis identifies loci for type 2 diabetes and triglyceride levels. *Science*, **316**, 1331–1336.
13. Scott, L.J., Mohlke, K.L., Bonnycastle, L.L., Willer, C.J., Li, Y., Duren, W.L., Erdos, M.R., Stringham, H.M., Chines, P.S., Jackson, A.U. *et al.* (2007) A genome-wide association study of type 2 diabetes in Finns detects multiple susceptibility variants. *Science*, **316**, 1341–1345.
14. Uno, S., Zembutsu, H., Hirasawa, A., Takahashi, A., Kubo, M., Akahane, T., Aoki, D., Kamatani, N., Hirata, K. and Nakamura, Y. (2010) A genome-wide association study identifies genetic variants in the CDKN2BAS locus associated with endometriosis in Japanese. *Nat. Genet.*, **42**, 707–710.

15. Voight, B.F., Scott, L.J., Steinthorsdottir, V., Morris, A.P., Dina, C., Welch, R.P., Zeggini, E., Huth, C., Aulchenko, Y.S., Thorleifsson, G. *et al.* (2010) Twelve type 2 diabetes susceptibility loci identified through large-scale association analysis. *Nat. Genet.*, **42**, 579–589.
16. Yasuno, K., Bilguvar, K., Bijlenga, P., Low, S.K., Krischek, B., Auburger, G., Simon, M., Krex, D., Arlier, Z., Nayak, N. *et al.* (2010) Genome-wide association study of intracranial aneurysm identifies three new risk loci. *Nat. Genet.*, **42**, 420–425.
17. Zeggini, E., Weedon, M.N., Lindgren, C.M., Frayling, T.M., Elliott, K.S., Lango, H., Timpson, N.J., Perry, J.R., Rayner, N.W., Freathy, R.M. *et al.* (2007) Replication of genome-wide association signals in UK samples reveals risk loci for type 2 diabetes. *Science*, **316**, 1336–1341.
18. Bei, J.X., Li, Y., Jia, W.H., Feng, B.J., Zhou, G., Chen, L.Z., Feng, Q.S., Low, H.Q., Zhang, H., He, F. *et al.* (2010) A genome-wide association study of nasopharyngeal carcinoma identifies three new susceptibility loci. *Nat. Genet.*, **42**, 599–603.
19. Shete, S., Hosking, F.J., Robertson, L.B., Dobbins, S.E., Sanson, M., Malmer, B., Simon, M., Marie, Y., Boisselier, B., Delattre, J.Y. *et al.* (2009) Genome-wide association study identifies five susceptibility loci for glioma. *Nat. Genet.*, **41**, 899–904.
20. Turnbull, C., Ahmed, S., Morrison, J., Pernet, D., Renwick, A., Maranian, M., Seal, S., Ghoussaini, M., Hines, S., Healey, C.S. *et al.* (2010) Genome-wide association study identifies five new breast cancer susceptibility loci. *Nat. Genet.*, **42**, 504–507.
21. Turnbull, C., Rapley, E.A., Seal, S., Pernet, D., Renwick, A., Hughes, D., Ricketts, M., Linger, R., Nsengimana, J., Deloukas, P. *et al.* (2010) Variants near DMRT1, TERT and ATF7IP are associated with testicular germ cell cancer. *Nat. Genet.*, **42**, 604–607.
22. Emanuele, E., Lista, S., Ghidoni, R., Binetti, G., Cereda, C., Benussi, L., Maletta, R., Bruni, A.C. and Politi, P. (2011) Chromosome 9p21.3 genotype is associated with vascular dementia and Alzheimer's disease. *Neurobiol. Aging*, **32**, 1231–1235.
23. Burd, C.E., Jeck, W.R., Liu, Y., Sanoff, H.K., Wang, Z. and Sharpless, N.E. (2010) Expression of linear and novel circular forms of an INK4/ARF-associated non-coding RNA correlates with atherosclerosis risk. *PLoS Genet.*, **6**, e1001233.
24. Folkersen, L., Kyriakou, T., Goel, A., Peden, J., Malarstig, A., Paulsson-Berne, G., Hamsten, A., Hugh, W., Franco-Cereceda, A., Gabrielsen, A. *et al.* (2009) Relationship between CAD risk genotype in the chromosome 9p21 locus and gene expression. Identification of eight new ANRIL splice variants. *PLoS One*, **4**, e7677.
25. Holdt, L.M., Beutner, F., Scholz, M., Gielen, S., Gabel, G., Bergert, H., Schuler, G., Thiery, J. and Teupser, D. (2010) ANRIL expression is associated with atherosclerosis risk at chromosome 9p21. *Arterioscler. Thromb. Vasc. Biol.*, **30**, 620–627.
26. Harismendy, O., Notani, D., Song, X., Rahim, N.G., Tanasa, B., Heintzman, N., Ren, B., Fu, X.D., Topol, E.J., Rosenfeld, M.G. *et al.* (2011) 9p21 DNA variants associated with coronary artery disease impair interferon-gamma signalling response. *Nature*, **470**, 264–268.
27. Shea, J., Agarwala, V., Philippakis, A.A., Maguire, J., Banks, E., Depristo, M., Thomson, B., Guiducci, C., Onofrio, R.C., Kathiresan, S. *et al.* (2011) Comparing strategies to fine-map the association of common SNPs at chromosome 9p21 with type 2 diabetes and myocardial infarction. *Nat. Genet.*, **43**, 801–805.
28. Yap, K.L., Li, S., Munoz-Cabello, A.M., Raguz, S., Zeng, L., Mujtaba, S., Gil, J., Walsh, M.J. and Zhou, M.M. (2010) Molecular interplay of the noncoding RNA ANRIL and methylated histone H3 lysine 27 by polycomb CBX7 in transcriptional silencing of INK4a. *Mol. Cell*, **38**, 662–674.
29. Congrains, A., Kamide, K., Oguro, R., Yasuda, O., Miyata, K., Yamamoto, E., Kawai, T., Kusunoki, H., Yamamoto, H., Takeya, Y. *et al.* (2012) Genetic variants at the 9p21 locus contribute to atherosclerosis through modulation of ANRIL and CDKN2A/B. *Atherosclerosis*, **220**, 449–455.
30. Pasmant, E., Laurendeau, I., Heron, D., Vidaud, M., Vidaud, D. and Bieche, I. (2007) Characterization of a germ-line deletion, including the entire INK4/ARF locus, in a melanoma-neural system tumor family: identification of ANRIL, an antisense noncoding RNA whose expression coclusters with ARF. *Cancer Res.*, **67**, 3963–3969.
31. Jarinova, O., Stewart, A.F., Roberts, R., Wells, G., Lau, P., Naing, T., Buerki, C., McLean, B.W., Cook, R.C., Parker, J.S. *et al.* (2009) Functional analysis of the chromosome 9p21.3 coronary artery disease risk locus. *Arterioscler. Thromb. Vasc. Biol.*, **29**, 1671–1677.
32. Cunnington, M.S., Santibanez Koref, M., Mayosi, B.M., Burn, J. and Keavney, B. (2010) Chromosome 9p21 SNPs associated with multiple disease phenotypes correlate with ANRIL expression. *PLoS Genet.*, **6**, e1000899.
33. Broadbent, H.M., Peden, J.F., Lorkowski, S., Goel, A., Ongen, H., Green, F., Clarke, R., Collins, R., Franzosi, M.G., Tognoni, G. *et al.* (2008) Susceptibility to coronary artery disease and diabetes is encoded by distinct, tightly linked SNPs in the ANRIL locus on chromosome 9p. *Hum. Mol. Genet.*, **17**, 806–814.
34. Johnson, A.D., Hwang, S.J., Voorman, A., Morrison, A., Peloso, G.M., Hsu, Y.H., Thanassoulis, G., Newton-Cheh, C., Rogers, I.S., Hoffmann, U. *et al.* (2013) Resequencing and clinical associations of the 9p21.3 region: a comprehensive investigation in the Framingham Heart Study. *Circulation*, **127**, 799–810.
35. Motterle, A., Pu, X., Wood, H., Xiao, Q., Gor, S., Liang Ng, F., Chan, K., Cross, F., Shohreh, B., Poston, R.N. *et al.* (2012) Functional analyses of coronary artery disease associated variation on chromosome 9p21 in vascular smooth muscle cells. *Hum. Mol. Genet.*, **21**, 4021–4029.
36. Liu, Y., Sanoff, H.K., Cho, H., Burd, C.E., Torrice, C., Mohlke, K.L., Ibrahim, J.G., Thomas, N.E. and Sharpless, N.E. (2009) INK4/ARF transcript expression is associated with chromosome 9p21 variants linked to atherosclerosis. *PLoS One*, **4**, e5027.
37. Mercer, T.R., Dinger, M.E. and Mattick, J.S. (2009) Long non-coding RNAs: insights into functions. *Nat. Rev. Genet.*, **10**, 155–159.
38. Hasler, R., Feng, Z., Backdahl, L., Spehlmann, M.E., Franke, A., Teschendorff, A., Rakyan, V.K., Down, T.A., Wilson, G.A., Feber, A. *et al.* (2012) A functional methylome map of ulcerative colitis. *Genome Res.*, **22**, 2130–2137.
39. Franke, A., McGovern, D.P., Barrett, J.C., Wang, K., Radford-Smith, G.L., Ahmad, T., Lees, C.W., Balschun, T., Lee, J., Roberts, R. *et al.* (2010) Genome-wide meta-analysis increases to 71 the number of confirmed Crohn's disease susceptibility loci. *Nat. Genet.*, **42**, 1118–1125.
40. Divaris, K., Monda, K.L., North, K.E., Olshan, A.F., Lange, E.M., Moss, K., Barros, S.P., Beck, J.D. and Offenbacher, S. (2012) Genome-wide association study of periodontal pathogen colonization. *J. Dent. Res.*, **91**, S21–S28.
41. Schaefer, A.S., Richter, G.M., Nothnagel, M., Manke, T., Dommisch, H., Jacobs, G., Arlt, A., Rosenstiel, P., Noack, B., Groessner-Schreiber, B. *et al.* (2010) A genome-wide association study identifies GLT6D1 as a susceptibility locus for periodontitis. *Hum. Mol. Genet.*, **19**, 553–562.
42. Zabaneh, D. and Balding, D.J. (2010) A genome-wide association study of the metabolic syndrome in Indian Asian men. *PLoS One*, **5**, e11961.
43. Lemaitre, R.N., Tanaka, T., Tang, W., Manichaikul, A., Foy, M., Kabagambe, E.K., Nettleton, J.A., King, I.B., Weng, L.C., Bhattacharya, S. *et al.* (2011) Genetic loci associated with plasma phospholipid n-3 fatty acids: a meta-analysis of genome-wide association studies from the CHARGE Consortium. *PLoS Genet.*, **7**, e1002193.
44. Dupuis, J., Langenberg, C., Prokopenko, I., Saxena, R., Soranzo, N., Jackson, A.U., Wheeler, E., Glazer, N.L., Bouatia-Naji, N., Gloyn, A.L. *et al.* (2010) New genetic loci implicated in fasting glucose homeostasis and their impact on type 2 diabetes risk. *Nat. Genet.*, **42**, 105–116.
45. Mayor, C., Brudno, M., Schwartz, J.R., Poliakov, A., Rubin, E.M., Frazer, K.A., Pachter, L.S. and Dubchak, I. (2000) VISTA: visualizing global DNA sequence alignments of arbitrary length. *Bioinformatics*, **16**, 1046–1047.
46. Pandey, R.R., Mondal, T., Mohammad, F., Enroth, S., Redrup, L., Komorowski, J., Nagano, T., Mancini-Dinardo, D. and Kanduri, C. (2008) Kcnq1ot1 antisense noncoding RNA mediates lineage-specific transcriptional silencing through chromatin-level regulation. *Mol. Cell*, **32**, 232–246.
47. Yamauchi, T., Nio, Y., Maki, T., Kobayashi, M., Takazawa, T., Iwabu, M., Okada-Iwabu, M., Kawamoto, S., Kubota, N., Kubota, T. *et al.* (2007) Targeted disruption of AdipoR1 and AdipoR2 causes abrogation of adiponectin binding and metabolic actions. *Nat. Med.*, **13**, 332–339.
48. Stefan, N., Bunt, J.C., Salbe, A.D., Funahashi, T., Matsuzawa, Y. and Tataranni, P.A. (2002) Plasma adiponectin concentrations in children: relationships with obesity and insulinemia. *J. Clin. Endocrinol. Metab.*, **87**, 4652–4656.
49. Yang, W.S., Lee, W.J., Funahashi, T., Tanaka, S., Matsuzawa, Y., Chao, C.L., Chen, C.L., Tai, T.Y. and Chuang, L.M. (2001) Weight reduction increases plasma levels of an adipose-derived anti-inflammatory protein, adiponectin. *J. Clin. Endocrinol. Metab.*, **86**, 3815–3819.
50. Ceddia, R.B., Somwar, R., Maida, A., Fang, X., Bikopoulos, G. and Sweeney, G. (2005) Globular adiponectin increases GLUT4 translocation and glucose uptake but reduces glycogen synthesis in rat skeletal muscle cells. *Diabetologia*, **48**, 132–139.

51. Fu, Y., Luo, N., Klein, R.L. and Garvey, W.T. (2005) Adiponectin promotes adipocyte differentiation, insulin sensitivity, and lipid accumulation. *J. Lipid. Res.*, **46**, 1369–1379.
52. Ouchi, N., Kihara, S., Arita, Y., Maeda, K., Kuriyama, H., Okamoto, Y., Hotta, K., Nishida, M., Takahashi, M., Nakamura, T. *et al.* (1999) Novel modulator for endothelial adhesion molecules: adipocyte-derived plasma protein adiponectin. *Circulation*, **100**, 2473–2476.
53. Kraus, D., Winter, J., Jepsen, S., Jager, A., Meyer, R. and Deschner, J. (2012) Interactions of adiponectin and lipopolysaccharide from *Porphyromonas gingivalis* on human oral epithelial cells. *PLoS One*, **7**, e30716.
54. Kumada, M., Kihara, S., Ouchi, N., Kobayashi, H., Okamoto, Y., Ohashi, K., Maeda, K., Nagaretani, H., Kishida, K., Maeda, N. *et al.* (2004) Adiponectin specifically increased tissue inhibitor of metalloproteinase-1 through interleukin-10 expression in human macrophages. *Circulation*, **109**, 2046–2049.
55. Yokota, T., Oritani, K., Takahashi, I., Ishikawa, J., Matsuyama, A., Ouchi, N., Kihara, S., Funahashi, T., Tenner, A.J., Tomiyama, Y. *et al.* (2000) Adiponectin, a new member of the family of soluble defense collagens, negatively regulates the growth of myelomonocytic progenitors and the functions of macrophages. *Blood*, **96**, 1723–1732.
56. Murray, R.Z., Kay, J.G., Sangermani, D.G. and Stow, J.L. (2005) A role for the phagosome in cytokine secretion. *Science*, **310**, 1492–1495.
57. Schwenk, R.W., Luiken, J.J., Bonen, A. and Glatz, J.F. (2008) Regulation of sarcolemmal glucose and fatty acid transporters in cardiac disease. *Cardiovasc. Res.*, **79**, 249–258.
58. Schwenk, R.W., Angin, Y., Steinbusch, L.K., Dirkx, E., Hoebers, N., Coumans, W.A., Bonen, A., Broers, J.L., van Eys, G.J., Glatz, J.F. *et al.* (2012) Overexpression of Vesicle-associated Membrane Protein (VAMP) 3, but Not VAMP2, protects Glucose Transporter (GLUT) 4 protein translocation in an in vitro model of cardiac insulin resistance. *J. Biol. Chem.*, **287**, 37530–37539.
59. Do, R., Xie, C., Zhang, X., Mannisto, S., Harald, K., Islam, S., Bailey, S.D., Rangarajan, S., McQueen, M.J., Diaz, R. *et al.* (2011) The effect of chromosome 9p21 variants on cardiovascular disease may be modified by dietary intake: evidence from a case/control and a prospective study. *PLoS Med.*, **8**, e1001106.
60. Doria, A., Wojcik, J., Xu, R., Gervino, E.V., Hauser, T.H., Johnstone, M.T., Nolan, D., Hu, F.B. and Warram, J.H. (2008) Interaction between poor glycemic control and 9p21 locus on risk of coronary artery disease in type 2 diabetes. *JAMA*, **300**, 2389–2397.
61. Vermaak, W.J., Ubbink, J.B., Delport, R., Becker, P.J., Bissbort, S.H. and Ungerer, J.P. (1991) Ethnic immunity to coronary heart disease? *Atherosclerosis*, **89**, 155–162.
62. Westfall, P.H. and Young, S.S. (1993). *Resampling-based multiple testing: Examples and methods for P–value adjustment*, Wiley-Interscience, Vol. 279.
63. Purcell, S., Neale, B., Todd-Brown, K., Thomas, L., Ferreira, M.A., Bender, D., Maller, J., Sklar, P., de Bakker, P.I., Daly, M.J. *et al.* (2007) PLINK: a tool set for whole-genome association and population-based linkage analyses. *Am. J. Hum. Genet.*, **81**, 559–575.
64. Barrett, J.C., Fry, B., Maller, J. and Daly, M.J. (2005) Haploview: analysis and visualization of LD and haplotype maps. *Bioinformatics*, **21**, 263–265.